

### 5.3 Growth of High Quality AlN

Although the advantages of AlN in making waveguides are widely known, the fabrication of AlN waveguide has not been reported until now. This is because the growth of high quality AlN layer itself cannot be easily performed with the conventional growth technique using the same condition as that of GaN growth. In this section, the growth of AlN with the metalorganic vapor phase epitaxy (MOVPE) technique is therefore described.

Aluminum (Al) is well known for its fast reaction with oxygen, usually causing  $Al_xO_y$  layer being formed when  $O_2$  is mixed in the growth chamber. The growth of high quality AlN therefore requires  $H_2$  carrier gas that contains no  $O_2$  contamination. Such condition can be achieved in the MOVPE growth using Pd-cell purifier to produce the ultra-pure  $H_2$  carrier gas. Another well known chemical reaction of Aluminum is its parasitic reaction with  $NH_3$ . The parasitic reaction is the reaction occurred in the gas phase before reaching the substrate surface. It always occurs during the growth of nitride semiconductors especially for materials that contain Al, deteriorating the crystalline quality of the grown layer. In the growth of AlN layer, since only TMA is used for the group III, high rate of parasitic reaction is predictable, causing many difficulties in growing AlN with high crystalline quality. Basically, the cause of such high parasitic reaction rate is thought to be the fast reaction between the  $NH_3$  and TMA. The parasitic reaction can therefore be reduced by growing the AlN layer at low V/III ratio to reduce excess reaction between  $NH_3$  and TMA.

In addition to V/III ratio, the total flow rate of  $NH_3$  is one of the most important parameter that is needed to be concerned together with low V/III ratio. This is because the possibility that  $NH_3$  can meet with TMA in the gas phase can be reduced with decreasing  $NH_3$  flow rate, thus suppressing the excess parasitic reaction and improving the crystalline quality, as reported in the literature [173]. In this study, the effect of decreasing  $NH_3$  flow rate on the improvement of crystalline quality of AlN barrier in GaN/AlN MQW has been also confirmed previously, as already discussed in Chapter 2. For the growth of thick AlN layer, the flow rate of  $NH_3$  was therefore decreased to be as low as possible with the flow rate of  $NH_3$  of 150 sccm. Furthermore, the reactor

pressure was also decreased to be as low as 50 mbar, which is the lowest pressure that can be controlled with stability by MOVPE reactor used in this study.

In order to grow the AlN layer on sapphire substrate, the two-step growth technique was utilized using low-temperature (LT) AlN buffer layer. During the growth of AlN at high temperature, the flow rate of the TMA was set to 35  $\mu\text{mol}/\text{min}$ , corresponding to the V/III ratio as low as 200. The total flow rate during the growth of high-temperature AlN layer was approximately 10 standard litre per minute (slm). After finishing the growth of high-temperature AlN layer, all samples were slowly cooled down to room temperature, while keeping the same flow rate of  $\text{NH}_3$ , making it able to observe the surface morphology of the AlN layer.

Since the growth of AlN must be performed on the sapphire substrate in order to be used as cladding layer, the growth of low-temperature (LT) AlN layer is the most important process, as similar to the growth of GaN on sapphire substrate. The experiments were therefore performed on the (0001) sapphire substrate by changing the growth temperature of LT-AlN, ranging from 750  $^\circ\text{C}$  to 1050  $^\circ\text{C}$ , while the growth of latter high-temperature (HT) AlN was performed with the same growth temperature at 1240  $^\circ\text{C}$  for the thickness of 1  $\mu\text{m}$ . The characterization of crystalline quality by X-ray diffraction (XRD) measurements and surface morphology by Atomic Force Microscope (AFM) of 1.0- $\mu\text{m}$ -thick AlN with different growth conditions of LT-AlN buffer layer

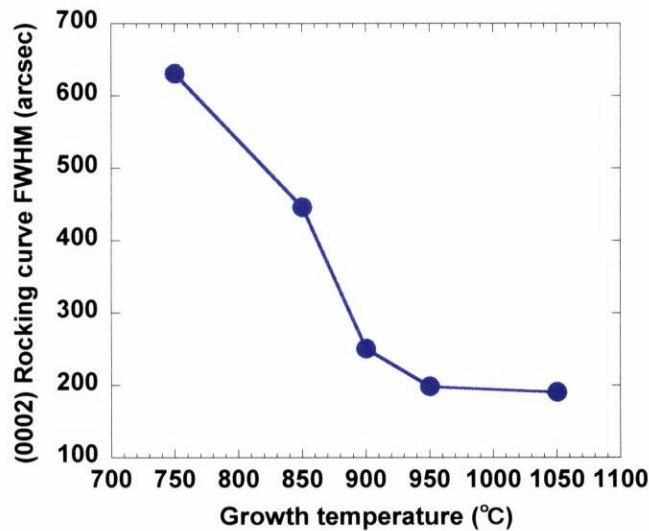


Figure 5.11 Full width at half maximum of (0002) AlN with rocking curve scan XRD as a function of LT-AlN growth temperature

revealed that the crystalline quality and surface morphology of AlN layers are strongly dependent on the growth temperature of LT-AlN buffer layer. Figure 5.11 shows the dependence of full-width at half-maximum (FWHM) of the XRD rocking curve for (0002) plane of AlN on the growth temperature of LT-AlN, while the surface morphology images taken by AFM are shown in Fig. 5.12. As seen in Fig. 5.11, the FWHM decreases with increasing growth temperature of LT-AlN buffer layer and becomes less than 200 arcsec when the growth temperature of LT-AlN is increased to above 900 °C. However, root-mean-square (RMS) surface roughness became worse with increasing temperature, as can be observed in Fig. 5.12. The optimal growth temperatures were finally found to be 900 °C for LT-AlN layer and 1240 °C for the growth of HT-AlN.

With the optimal condition, the growth of AlN was performed again for 2 μm to check the reproductivity. Figure 5.13 shows the XRD rocking curve scan of (0002) AlN. As can be seen in the figure, the sharp AlN peak with FWHM of 170 arcsec can be clearly observed, indicating that the growth of high-quality AlN layer on (0001) the sapphire substrate could be performed successfully. Figure 5.14 shows AFM surface morphology of the 1.0-μm-thick AlN buffer layer grown on (0001) sapphire substrate.

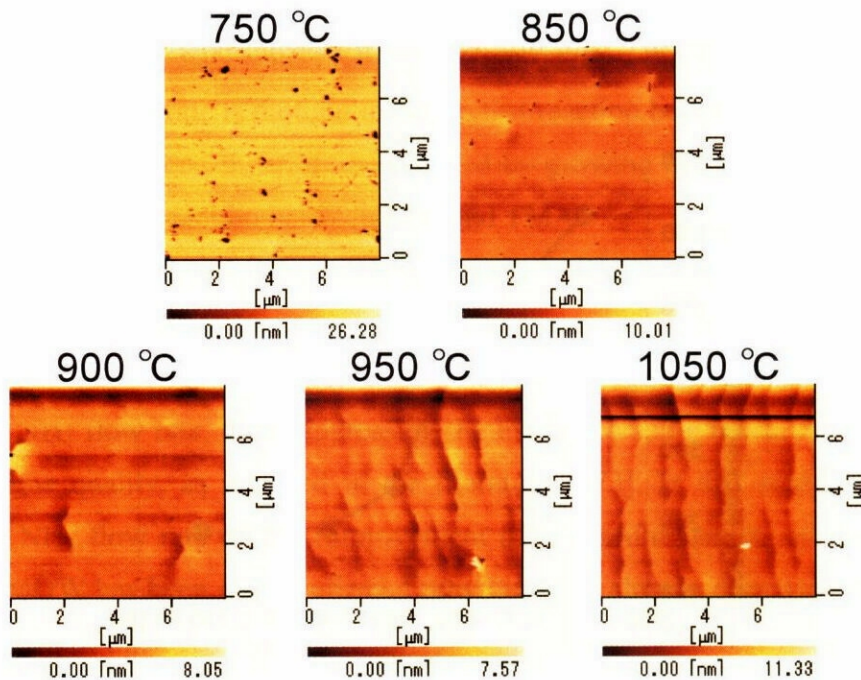


Figure 5.12 AFM surface morphologies of AlN with different growth temperature of low temperature AlN buffer layer

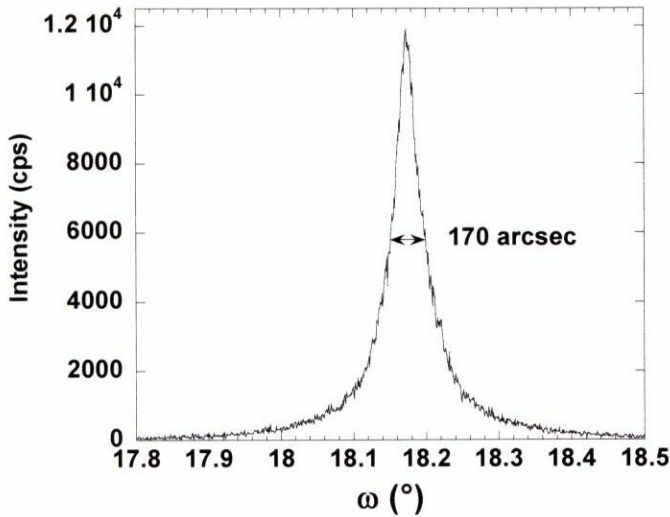


Figure 5.13 XRD rocking curve scan profile of (0002) AlN

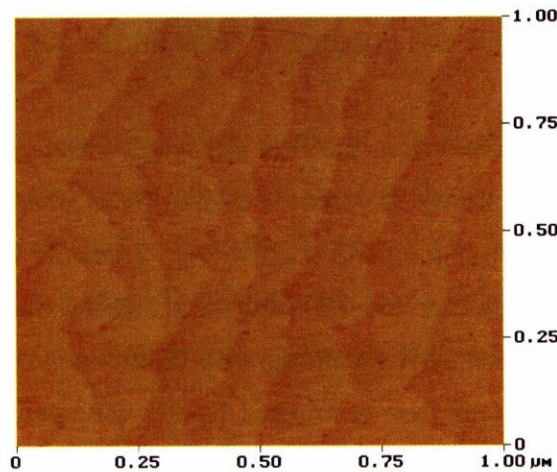


Figure 5.14 AFM surface morphology of AlN

The step-flow growth mode of AlN with the RMS surface roughness of 0.1 nm for  $1 \times 1 \mu\text{m}^2$  was clearly observed, showing very flat surface of AlN layer. The quality of this AlN layer is excellent compared to those reported in literatures [173,174], indicating a big improvement of crystalline quality as a result of the careful control of oxygen contamination and V/III ratio along with the optimization of growth temperatures. With these results, it has been confirmed that the AlN layer has good crystalline quality and very flat surface, suitable for fabrication of AlN cladding layer in the waveguide structures.

## 5.4 Fabrication of AlN High-Mesa Waveguides

After achieving the high-quality AlN buffer layer on sapphire substrate described in the last section, the fabrication of AlN-based waveguides was also demonstrated for the first time in this study using ICP etching technique. The waveguide patterns were formed by photolithography using SiO<sub>2</sub> as etching mask, as same as that of GaN etching process which is already described in Chapter 4. The ICP etching was performed using the same pressure and gas flow rate: Pressure 7 Pa, Cl<sub>2</sub> 8 sccm, Ar 2 sccm, while the ICP power and bias power were increased to 600 W and 250 W, respectively. With this etching condition, the AlN-based high-mesa waveguides were successfully fabricated with the etching rate of approximately 125 nm per minute, which is a little bit dropped from GaN etching rate. After finished etching of AlN, the SiO<sub>2</sub> etching mask was removed by buffer HF. Then the wafer was grinding to be as thin as 100 μm before polishing to get mirror-like surface.

With such etching condition, the first AlN high-mesa waveguide was successfully fabricated. Figure 5.15 shows the cross-sectional SEM image of the waveguide which was cleaved to be 500 μm long. As seen in Fig. 5.15, the high-mesa waveguide with good sidewall and smooth surface are achieved, showing that the etching of AlN could be successfully performed by ICP etching with such condition. The light propagation in high-mesa waveguides was then confirmed by the waveguide measurements using the

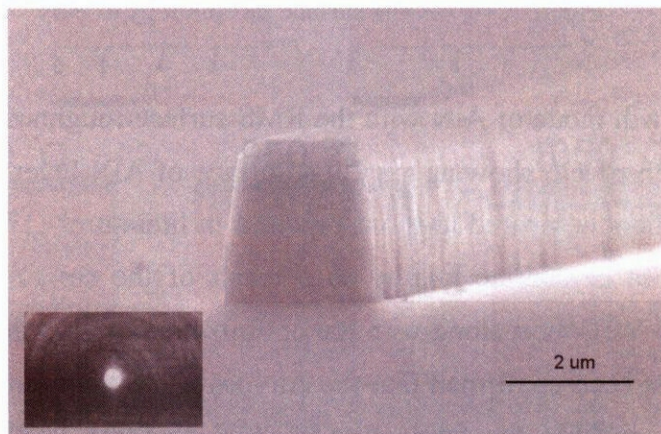


Figure 5.15 Cross sectional SEM image of high-mesa AlN waveguide  
Inset: near-field image of propagated light at 1.55 μm

same measurement system as that of Fig. 4.12. Inset of Figure 5.15 shows the near-field view of the propagated light taken by an infrared camera. Obviously, it can be seen that the light propagation for 1.55  $\mu\text{m}$  has been confirmed with round beam, indicating that the waveguide is successfully fabricated.

In order to investigate quality of the waveguides, Fabry-Perot Etalon method was firstly used. By measuring the length of one period of Fabry-Perot interference, the propagation loss can be calculated by the following equation:

$$\alpha = -\frac{1}{l} \ln \left( \frac{1}{R} \cdot \frac{\sqrt{H} - 1}{\sqrt{H} + 1} \right) \quad (5.1)$$

where  $H$  is peak to valley ratio, and  $R$  is reflectance of the waveguide facet. The effective reflectance of the waveguide facet can be also calculated by

$$H = \frac{T_{\max}}{T_{\min}} = \frac{(1 + R')^2}{(1 - R')^2} \quad (5.2)$$

The propagation loss for TM and TE mode of the as-fabricated AlN high-mesa waveguide estimated by Fabry-perot etalon method is shown in Table 5.1. As can be seen in the Table, the propagation loss for TM and TE mode is estimated to be approximately 10 dB/cm and there is no big difference between TM and TE mode, suggesting that the extra propagation loss caused by crystalline defects is quite small.

Table 5.1 Propagation loss of AlN waveguide measured by Fabry-perot etalon method

Waveguide width	Propagation Loss	
	TM mode	TE mode
2 $\mu\text{m}$	10 dB/cm	11.1 dB/cm
3 $\mu\text{m}$	11 dB/cm	9.7 dB/cm

To confirm this loss, the waveguides were characterized by the Supercontinuum Light source, using the same experimental setup shown in Fig. 4.13. Figure 5.16 shows the light transmission of TM mode compared to TE mode. With waveguide length of around 500  $\mu\text{m}$ , the measurements show no big difference in transmission intensity between TM and TE mode, indicating that the waveguide has good crystalline quality and does not generate the addition TM mode loss. This clearly shows that the AlN

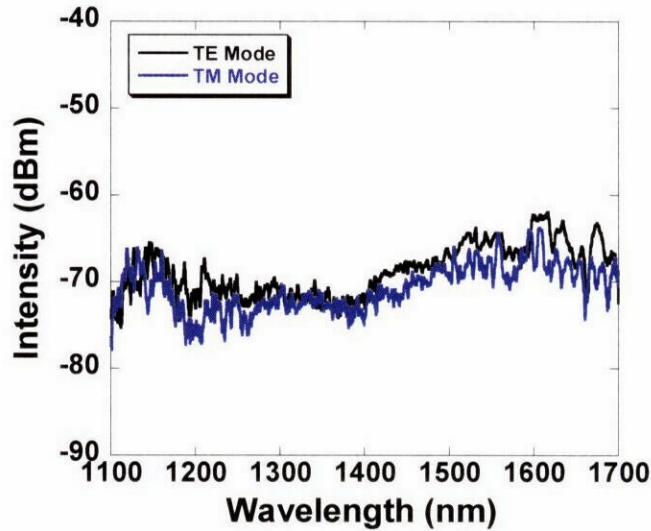


Figure 5.16 TM and TE mode transmission spectra measured by waveguide coupling method with supercontinuum light source

waveguide structure grown by MOVPE was successfully fabricated with very high quality, suitable for the intersubband absorption devices.

## 5.5 Fabrication of AlN Waveguides with GaN Guiding Layer

The other structure that is proposed in this study is the high optical confinement structure of AlN waveguide. The waveguide contains the GaN guiding layer to increase the effective refractive index of the core part. In order to fabricate such structure, first of all, the problem concerning the growth has to be overcome. This is because the large lattice mismatch between AlN and GaN (~2.6%) can generate high density of dislocations and cracks, which always make difficulty in obtaining good crystalline quality. This section therefore describes the fabrication of AlN waveguide with GaN guiding layers beginning with the growth of such structure with high crystalline quality by MOVPE growth technique.

After performing the growth of AlN layer using the optimal condition demonstrated in the last section, the reactor pressure and temperature were adjusted to the optimal condition for the growth of GaN to perform the growth of GaN guiding layer. Firstly,

GaN layer was grown directly on 1- $\mu\text{m}$ -thick AlN layer without any low-temperature buffer layer. However, the surface morphology taken by AFM contains quantum-dot-like defects is observed, which are thought to be caused by the large lattice mismatch between GaN and AlN, inducing three-dimensional growth mode of GaN as reported in the literature [175]. Considering this result, it is therefore not possible to grow more layers of MQW on this GaN layer.

In order to obtain a good crystalline quality GaN layer, the growth of such structure therefore requires special growth technique to suppress the stress generated in the GaN during growing on AlN. Such structure was therefore grown with the two-step growth technique using low-temperature GaN buffer layer, as same as the GaN buffer layer grown on sapphire substrate. After finishing the growth of 1- $\mu\text{m}$ -thick AlN layer, the reactor pressure and temperature were set to 200 mbar and 550  $^{\circ}\text{C}$ , respectively, the optimal growth condition for low-temperature GaN buffer layer. Using such condition, the growth rate increased to be 2 times faster than that of normal growth of low-temperature GaN on sapphire substrate. This phenomenon is considered to be a result of a decrease in lattice mismatch from 17% (with sapphire substrate) to be around 2.6% (with AlN buffer layer). The thickness of this low-temperature GaN buffer layer was, however, set to be around 25 nm, as same as those grown on sapphire substrates, before growing the GaN at 1150  $^{\circ}\text{C}$  with thickness around 400 nm. The growth of GaN

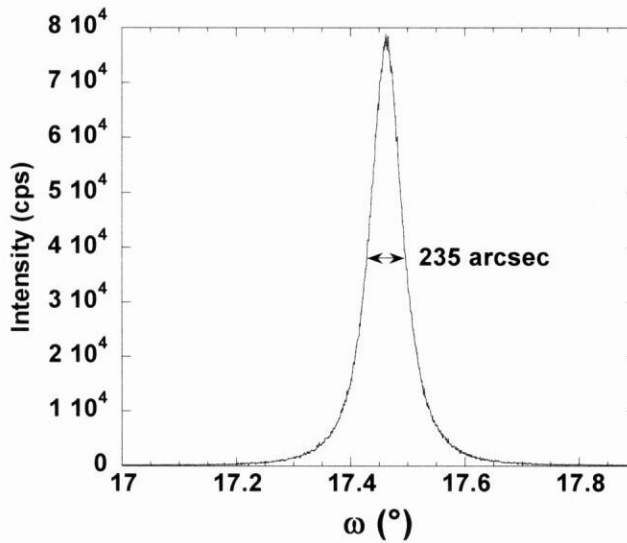


Figure 5.17 XRD rocking curve scan profile of (0002) GaN grown on AlN with LT-GaN buffer layer technique

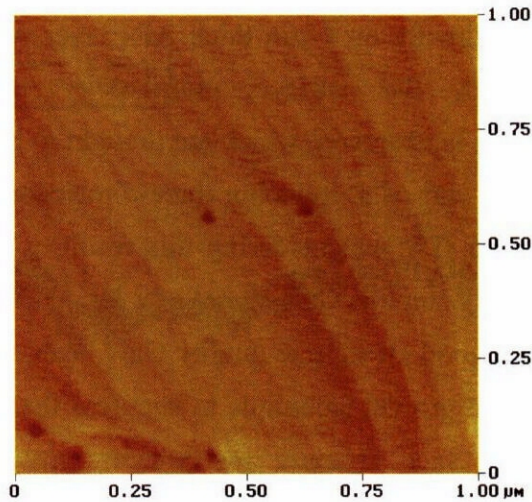


Figure 5.18 AFM surface morphology of GaN grown on AlN with LT-GaN buffer layer technique

with this two-step growth technique could improve the crystalline quality and surface morphology as can be seen in XRD rocking curve results and AFM image shown in Fig. 5.17 and Fig. 5.18, respectively. These results suggest that the GaN/AlN MQW could be grown on this GaN layer to make the optical devices.

Next, the growth of GaN/AlN MQW has been performed on the GaN layer which was successfully grown AlN buffer layer. The growth temperature and reaction pressure during the growth of MQW layer was set to be 1100°C and 60 mbar, respectively. The

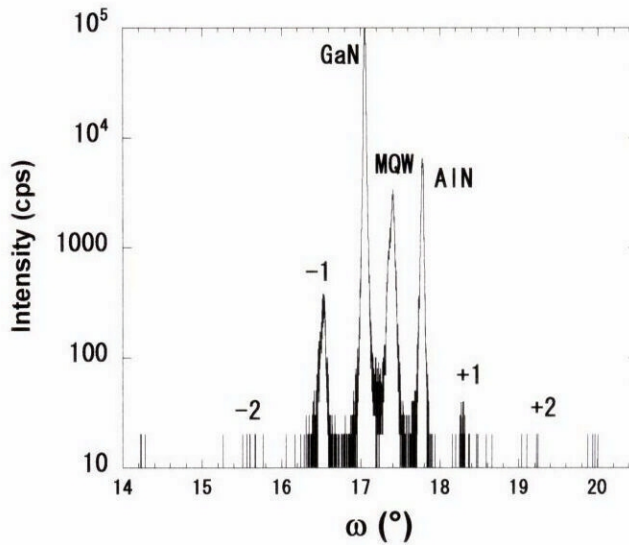


Figure 5.19 XRD  $\omega/2\theta$  scan profile of 40-period GaN/AlN MQW grown on GaN-AlN buffer with LT buffer layer technique

MQW structure composed of 40 periods of GaN quantum wells and AlN barrier, with thickness of 2.5 nm and 2.0 nm, respectively. The structural quality of MQW was then characterized by XRD measurements with  $\omega/2\theta$  scan as shown in Fig. 5.19. As can be seen, the satellite peaks up to  $-2^{\text{nd}}$  order was clearly observed, confirming that the structural quality of the MQW layer was very good. The surface morphology observed by Nomarsky microscope shows that cracking was generated on the sample surface. However, the cracking was thought to be generated as the MQW layer contains many quantum wells with thickness of around 200 nm, obviously thicker than the critical thickness of GaN/AlN MQW on GaN layer. This cracking is however considered to not causing any problem in the observation of intersubband transition at this stage. The intersubband absorption measurements in the as-grown MQW were therefore performed by Multiple-reflection method. Figure 5.20 shows the transmission spectrum of p-polarized light taken for the as-grown MQW Multiple-reflection waveguide with a length of 6 mm. Clearly the intersubband absorption was observed with the peak wavelength of 2.7  $\mu\text{m}$ . The full-width at half-maximum was estimated to be around 100 meV. As the intersubband absorption was observed in such structure, it was made sure that the structure was grown with high quality, and such structure is applicable for the fabrication of optical waveguides.

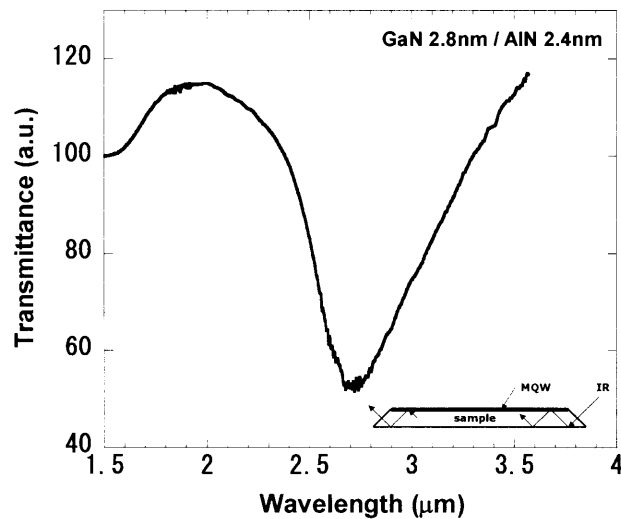


Figure 5.20 Transmission spectrum of 40-period GaN(2.8nm)/AlN(2.4nm) MQW on GaN-AlN buffer layer measured by Multiple-reflection method

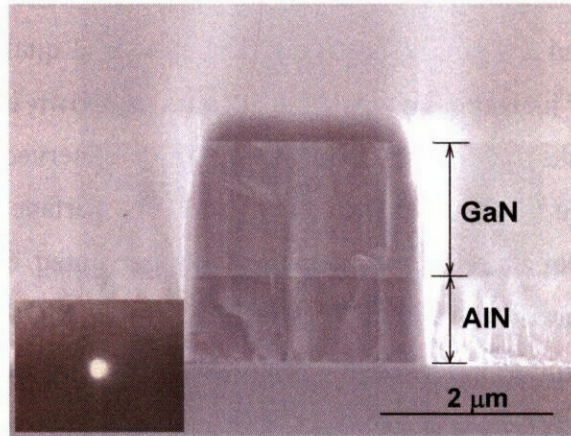


Figure 5.21 Cross sectional SEM image of AlN-clad GaN waveguide  
Inset: near-field image of propagated light at 1.55  $\mu\text{m}$

In order to demonstrate the high-confinement waveguide structure, the waveguide fabrication was performed for a structure composed of 2- $\mu\text{m}$ -thick GaN layer stacked on 1- $\mu\text{m}$ -thick AlN layer. As mentioned in Chapter 5.3, growing the upper AlN cladding layer requires high temperature growth that could destroy the crystalline and structural quality of the previously grown GaN layer. The upper AlN cladding layer was not fabricated in this experiment to avoid raising the growth temperature. The waveguide fabricated in this section is therefore the same as one in Section 5.2.3. The  $\text{SiO}_2$  sputtering and photolithography process was used to make the  $\text{SiO}_2$  etching-mask patterns, while the etching was carried out by the ICP etching technique using mixture of  $\text{Cl}_2$  and Ar. The pressure of etching chamber was set to be 7 Pa during etching process with the ICP power and bias power of 300 W and 175 W, respectively. Figure 5.21 shows the cross-sectional SEM image of as fabricated waveguide. It can be seen in the figure that the high-mesa waveguide could be successfully fabricated as the etching was performed until the sapphire surface. As seen in the figure, some damage was observed at the upper of the waveguide sidewall, because the edge of  $\text{SiO}_2$  mask was firstly damaged when the etching was performed for a period of time. Nevertheless, this could not affect much with the propagation mode of the waveguide, as smooth sidewall of the waveguide and perpendicular angle to sapphire substrate were obtained.

Inset in Fig. 5.21 shows the near-field view of the propagated light for 1.55  $\mu\text{m}$ . Clear and round beam was observed, indicating that the waveguide is successfully fabricated and it is ready for the fabrication of the optical waveguide. Though the waveguide contains no upper cladding layer, it can be seen that the waveguide could be used very well with such structure. The waveguide characteristic, however, might be improved by depositing the cladding layer with other processes such as sputtering or spin coating, which is much easier compared to the growth of thick AlN layer. These results show that the high-optical-confinement AlN waveguide with GaN guiding layer could be fabricated with high quality, suitable for the further development of optical waveguides toward the improvement of intersubband transition devices.

## 5.6 Concluding Remarks

In this chapter, the AlN-based waveguide structures were proposed and fabricated. It was found out by simulation that using the AlN as cladding layers can improve the optical confinement of the waveguide. Moreover, the AlN has many advantages for fabrication of intersubband transition devices, for example, good carrier confinement, strong built-in electric field, low refractive index and low reflectance.

Three kinds of high-optical-confinement waveguide structures were therefore designed and studied for the waveguide fabrication in Section 5.2. In order to demonstrate the fabrication of designed structures, in Section 5.3, the epitaxial growth of high crystalline quality AlN was performed by MOVPE with two-step growth technique at low pressure of 60 mbar. The most important parameter for the growth of AlN by MOVPE is the V/III ratio, which should be low to suppress the parasitic reaction between  $\text{NH}_3$  and Al. Moreover, it was found that the crystalline quality and the surface roughness of the AlN layer is very sensitive to the temperature of low-temperature AlN buffer layer. The optimized temperatures were found out to be 900  $^\circ\text{C}$  and 1240  $^\circ\text{C}$  for LT-AlN and HT-AlN, respectively. With the optimal growth condition, high quality AlN layer up to 2  $\mu\text{m}$  can be successfully grown on sapphire substrate.

In Section 5.4, the fabrication of high quality AlN waveguide was demonstrated using the inductively coupled plasma etching technique. The optimized ICP power and bias power were found to be 600 W and 250 W, respectively. Then, the fabrication of high-mesa waveguide was successfully performed with such etching condition. The waveguide provides low propagation loss for both TM and TE polarization, confirmed by the Fabry-perot etalon method and the new waveguide characterization by supercontinuum light source, indicating very good waveguide quality suitable for the realization of intersubband transition devices.

Furthermore, the growth of high-optical-confinement waveguide structure with GaN guiding layer was demonstrated with metalorganic vapor phase epitaxy using two-step growth technique for each layer. The growth was performed successfully, confirmed by AFM, XRD and intersubband absorption measurements. Then, the fabrication of such high-optical-confinement was successfully fabricated with the inductively coupled plasma etching technique, confirming that this waveguide structure can be fabricated with high quality and is expected to be another candidate of waveguide structures for the realization of low-switching-energy ultrafast all-optical switch utilizing intersubband transition.